J. Biochem. **137**, 463–476 (2005)
DOI: 10.1093/jb/mvi054

Alterations in the Extracellular Matrix Proteoglycan Profile in Dupuytren's Contracture Affect the Palmar Fascia

Ewa Maria Koźma, Krystyna Olczyk*, Grzegorz Wisowski, Andrzej Głowacki and Rafał Bobiński

Department of Clinical Chemistry and Laboratory Diagnostics, Medical University of Silesia, ul. Jagiellońska 4, 41-200 Sosnowiec, Poland

Received November 11, 2004; accepted December 30, 2004

Dupuytren's disease is a palmar fibromatosis associated with changes in fibroblast activity that also affect the metabolism of extracellular matrix components. In contrast to disease connected alterations in collagen and non-collagenous glycoproteins (mainly fibronectin), the metabolism of proteoglycans, being glycosaminoglycan modified glycoproteins, is poorly understood. Thus, the aim of the present study was the characterization of matrix proteoglycans (PGs) derived from normal fascia and Dupuytren's fascia. Extracted and purified PGs (particularly small PGs) were analysed for content, molecular mass, immunoreactivity and glycosaminoglycan chain structure. The matrix of normal fascia mainly contains decorin [small dermatan sulfate (DS) PG] with biglycan (another small DSPG) and large chondroitin sulfate(CS)/DSPG representing minor components. Dupuytren's disease is associated with the remodeling of matrix PG composition. The most prominent alteration is an accumulation of biglycan frequently bearing DS chains with higher molecular masses. Moreover, the amount of large CS/DSPG is increased. In contrast, decorin displays changes affecting mainly DS chain structure reflected in (i) an increase in some chain molecular masses, (ii) an enhanced content of iduronate disaccharide clusters, and (iii) oversulfation of disaccharide repeats. The PG alterations observed in Dupuytren's fascia may influence the matrix properties and contribute to disease progression.

Key words: biglycan, decorin, dermatan sulfate, Dupuytren's contracture, large CS/DSPG.

Abbreviations: BSA, bovine serum albumin; CHAPS, 3-((3-cholamidopropyl)dimethylammonio)-1-propane-sulfonate; CS, chondroitin sulfate; C-4-S, chondroitin-4-sulfate; C-6-S, chondroitin-6-sulfate; CS/DSPG, chondroitin sulfate/dermatan sulfate proteoglycan; DS, dermatan sulfate; DF, Dupuytren's fascia; ECM, extracellular matrix; EDTA, ethylenediaminetetraacetic acid disodium salt dihydrate; FGF, fibroblast growth factor; GAG, glycosaminoglycan; Gal, galactose; GalNAc, *N*-acetyl galactosamine; GlcA, glucuronic acid; GlcNAc, *N*-acetyl glucosamine; $GlcNSO_3^-$, *N*-sulfo glucosamine; GdnHCl, guanidine HCl; ΔHexA, 4-deoxy-L-threo-hex-4-enopyranosyluronic acid; IdoA, iduronic acid; NF, normal fascia; PDGF, platelet derived growth factor; PG, proteoglycan; PMSF, phenylmethanesulfonyl fluoride; SDS-PAGE, sodium dodecyl sulfate–polyacrylamide gel electrophoresis; TBS, tris buffered saline; TCA, trichloroacetic acid; TGFβ, transforming growth factor β.

Proteoglycans (PGs) are glycosaminoglycan (GAG) modified glycoproteins that are widespread in animal tissues. The molecules exist intracellularly, on the cell surface as well as in the extracellular matrix (ECM). Matrix PGs represent a heterogenous group of macromolecules characterized by various types of GAG chains attached to structurally different, multidomain core proteins (*1*). Matrix PG functions can be divided into three categories: (i) participation in ECM assembly *via* binding to collagens, elastin, non-collagenous glycoproteins and hyaluronic acid, (ii) influence on matrix permeability, and (iii) actions on cell behaviour by means of growth factor and cytokine sequestering in the ECM, as well as interactions with various cell receptors followed by signalling. The fulfilment of these specific functions depends upon linking miscellaneous ligands to the PG core protein and/or to GAG chains. The latter represent unbranched sulfated heteropolisaccharides that are polymers of disaccharide repeats. However, the disaccharide unit composition differs in various types of sulfated GAGs. Heparan sulfate and heparin are co-polymers of disaccharides including D-glucuronate and *N*-acetyl/*N*-sulfo glucosamine residues (GlcA-GlcNAc/$GlcNSO_3^-$) or L-iduronate and *N*-sulfo/*N*-acetyl glucosamine residues (IdoA-$GlcNSO_3^-$/GlcNAc), respectively (*2*). Dermatan sulfate (DS) also comprises two types of disaccharide repeats: D-glucuronate-*N*-acetyl galactosamine (GlcA-GalNAc) and L-iduronate-*N*-acetyl galactosamine (L-IdoA-GalNAc) (*3*). On the other hand, chondroitin sulfate (CS) and keratan sulfate are formed by only one kind of monomer, including D-glucuronate and *N*-acetyl galactosamine residues (GlcA-GalNAc) or D-galactose and *N*-acetyl glucosamine residues (Gal-GlcNAc), respectively (*3*). However, all sulfated GAGs display remarkable structural diversity due to different chain lengths as well as various patterns of sulfation and/or C-5-uronosyl epimerisation (conversion of glucuronic to iduronic acid occurring in co-polymeric GAG chains) (*3*). The GAG structure and/or expression of

*To whom correspondence should be addressed. Phone: +48-32-2924795, Fax: +48-32-2924795, E-mail: chem_klin@farmant.slam.katowice.pl

Table 1. **Information about tissue samples and their donors.**

Symbol	Kind of tissue	Sex	Age	Mode of sample handling
K1	normal fascia from two hands	M	42	separately
K2	normal fascia from two hands	M	55	separately
K3	normal fascia from two hands	M	69	separately
K4	normal fascia	F	35	separately
K5	normal fascia	F	43	separately
K6	normal fascia from two hands	F	48	separately
K7	normal fascia from two hands	F	54	separately
K8/9	normal fascia	F	50	combined in equal proportion with K9 due to small amount of tissue
K8/9	normal fascia	F	52	combined in equal proportion with K8 due to small amount of tissue
K10	normal fascia from two hands	F	58	separately
K11/12	normal fascia	F	60	combined in equal proportion with K12 due to small amount of tissue
K11/12	normal fascia	F	60	combined in equal proportion with K11 due to small amount of tissue
K13	normal fascia from two hands	F	64	separately
K14	normal fascia	F	69	separately
D1	Dupuytren's fascia	M	43	separately
D2	Dupuytren's fascia	M	44	separately
D3	Dupuytren's fascia	M	46	separately
D4	Dupuytren's fascia	M	49	separately
D5	Dupuytren's fascia	M	50	separately
D6	Dupuytren's fascia	M	53	separately
D7	Dupuytren's fascia	M	54	separately
D8	Dupuytren's fascia	M	56	separately
D9	Dupuytren's fascia	M	72	separately
D10	Dupuytren's fascia	M	73	separately
D11	Dupuytren's fascia	M	74	separately
D12	Dupuytren's fascia	F	49	separately
D13	Dupuytren's fascia	F	54	separately
D14	Dupuytren's fascia	F	60	separately
D15	Dupuytren's fascia	F	67	separately

PG core proteins depend upon the action of partly known factors, including cytokines and growth factors (*4*, *5*) as well as collagen (*6*). The complex system of PG metabolism affecting factors changes under various physiological and pathological conditions leading to the formation of a specific matrix PG profile. These poorly known changes in matrix PGs may be involved in the pathogenesis of various diseases.

Dupuytren's disease is mainly a palmar fibromatosis leading to progressive digital flexion contracture (*7*). In the course of the disease, two types of lesions are observed to co-exist in the palmar fascia—nodules consisted of proliferating fibroblasts/myofibroblasts and contracted collagenous cords (*7*). The former structures represent the early stage of the disease, and the latter are typical of the advanced disease (*7*). In the pathogenesis of Dupuytren's contracture, a key role is played by changes in palmar fascia fibroblast activity that occur probably as a result of high levels of growth factors [mainly transforming growth factor β1 (TGF β1), fibroblast growth factor–2 (FGF-2), platelet derived growth factor (PDGF)] and free radicals (for reviews: *8–10*). The abnormal cell behaviour is manifested by (i) intensive proliferation activity, (ii) the appearance of a myofibroblast phenotype characterized by the presence of α-actin microfilament bundles in the cytoplasm, and (iii) alterations in the synthesis of ECM components. Changes in collagen and noncollagenous glycoproteins connected with Dupuytren's disease are already known, while the PG metabolism is poorly understood. Thus, the aim of the present study was an evaluation of Dupuytren's fascia (DF) matrix PGs.

MATERIALS AND METHODS

Materials—Urea, guanidine HCl, all protease inhibitors, Sepharose CL-4B, CHAPS [3-((3-cholamidopropyl)dimethylammonio)-1-propane-sulfonate], Tween 20, glycine, papain, acrylamide, Azur A, chondroitinase ABC [EC 4.2.2.4] from *Proteus vulgaris*, chondroitinase B from *Flavobacterium heparinum*, bovine testicular hyaluronidase [EC 3.2.1.35], electrotransfer markers and Immobilon-P transfer membranes of Millipore were supplied by Sigma-Aldrich Chemie GmbH, Steinheim, Germany. Tris [tris(hydroxymethyl)aminomethane], dimethylmethylene blue, Coomassie Blue R250, *N,N′*-methylenebisacrylamide, molecular mass markers, as well as reference dermatan sulfate from pig skin and reference chondroitin-4-sulfate from whale cartilage were obtained from Serva Feinbiochemica GmbH, Heidelberg, Germany. DEAE-Sephacel and octyl Sepharose CL-4B were purchased from Pharmacia Biotech, Uppsala, Sweden. Sodium dodecyl sulfate and *N,N,N′,N′′*-tetramethylethylenediamine were supplied by ICN Biomedicals, Inc., Aurora, OH, USA. Blot Quick Blocker was obtained from Chemicon International, Temecula, CA, USA. Chondroitinase AC [EC 4.2.2.5] from *Flavobacterium heparinum* was purchased from Seikagaku Corporation, Tokyo, Japan. All others chemicals were supplied by Polskie

Odczynniki Chemiczne, Gliwice, Polska and were of analytical grade.

Tissue Material—Samples of normal (unaffected) palmar fascia (NF) were taken during hand-surgery from 14 patients (11 women, 3 men; age range 35 to 69 years) suffering from non-rheumatoid carpal tunnel syndrome. Specimens of DF were obtained from 15 patients (4 women, 11 men; age range 43 to 74 years) treated operatively for this disease. Specimens of DF were mainly in the fibrotic stage according to criteria set forward by Rombouts *et al.* (*11*) as evaluated by conventional histology. Treatment at this phase of the disease gives a low risk of recurrence. Tissue donor characteristics, including the mode of tissue sample handling are given in Table 1. All tissue samples were obtained with informed consent of the patients. The study protocol was approved by the Regional Ethical Committee. The specimens, freed from adjacent tissues, were stored at –20°C until processing.

Proteoglycan Extraction and Purification—Weighed tissue samples were homogenized in acetone in order to degrease and dehydrate and then reweighed. The samples were then suspended in buffer (10 ml/1 g dry tissue) containing 7.8 M urea in 0.05 M sodium acetate (pH 6.0) with 0.2 M NaCl and protease inhibitors (5 mM ethylmaleimide, 5 mM benzamidine HCl, 10 mM EDTA, 10 mM ε-amino-*n*-caproic acid and 1 mM PMSF). Matrix PGs were extracted for 24 h at 4°C under stirring. Extracts were separated from the tissue pellets by centrifugation (19,000 × *g*) and the extraction procedure was repeated. The combined extracts were applied to a DEAE-Sephacel column (5 ml bed volume) equilibrated and washed with 7.8 M urea in 0.05 M sodium acetate buffer, pH 6.0, containing 0.2 M NaCl, 0.25% (v/v) Triton X-100 and protease inhibitors in order to separate PGs from other molecules. The PGs/free sulfated GAGs bound to DEAE-Sephacel (anion exchanger) were eluted with equilibrating buffer containing 1 M NaCl and 0.1% (v/v) Triton X-100. The presence of PGs/free sulfated GAGs in 2 ml fractions was monitored by reaction with dimethylmethylene blue dye according to Farndale *et al.* (*12*). Fractions containing PGs/free sulfated GAGs were combined, dialyzed into 0.05 M sodium acetate, 0.1% (v/v) Triton X-100, and concentrated with Centriplus centrifugal concentrators (Amicon). Simultaneously with sample concentration, the buffer was changed to 4 M guanidine HCl (GdnHCl) in 0.15 M sodium acetate, pH 6.3. The prepared samples were further subjected to gel filtration in order to fractionate the PGs into large and small molecules. The chromatography was carried out on a 1 × 44 cm column of Sepharose CL-4B in 4 M GdnHCl, 0.15 M sodium acetate, pH 6.3. The column void volume (V_o) and total volume (V_t) were determined by the elution position of Blue Dextran and tyrosine, respectively. Fractions (0.5 ml) were eluted at a flow rate of 0.6 ml/min and analysed for PGs/free sulfated GAGs by the dimethylmethylene blue dye-binding assay (*12*). Fractions containing large and small PGs were combined and precipitated by the addition of 10 volumes of cold absolute ethanol followed by overnight incubation at 4°C. The PG pellets were collected by centrifugation (19,000 × *g*) and dried. After reconstitution of the pellets in distilled water, aliquots were taken for the determination of protein content according to Bradford (*13*). The remaining PG samples were frozen, lyophilized and stored at –20°C until analysed by sodium dodecyl sulfate–polyacrylamide gel electrophoresis (SDS-PAGE) and then by Western blotting. Samples containing small PGs (decorin and biglycan) were subsequently submitted to hydrophobic interaction chromatography on octyl-Sepharose CL-4B according to Choi *et al.* (*14*) to separate these glycoproteins. The column was equilibrated in 4 M GdnHCl, 0.15 M sodium acetate, pH 6.3, at 25°C. The volume of octyl-Sepharose used depended on the PG sample, so that the ratio of the bed volume to PG content was 7.5 ml/1 mg. After 2 h binding of PGs to the bed, decorin was eluted with equilibrating buffer as unbound material. Biglycan bound to octyl-Sepharose was eluted with 1% CHAPS in 4 M GdnHCl, 0.15 M sodium acetate. The purities of decorin and biglycan were assessed by SDS-PAGE and also by rechromatography on octyl-Sepharose CL-4B in the presence of 2 M GdnHCl (*14*). The molecules adsorbed to the bed were eluted using a linear gradient of 2–6 M GdnHCl. To confirm the purity of decorin and biglycan in the case of DF-derived PGs, Western blotting was carried out.

SDS-PAGE of Proteoglycans—To evaluate the PG profile of palmar fascia extracts, the molecules fractionated by gel filtration were further subjected to 7% or 4–15% SDS-PAGE before and after treatment with chondroitinase ABC. Enzyme digestion of CS/DS chains in order to release the PG core proteins was carried out as described previously (*15*). To check the sensitivity of small PGs to heparitinase, the molecules were subjected to the enzyme action as described previously (*15*). The electrophoresis of core proteins and intact PGs was performed according to Laemmli (*16*) using Sigma apparatus. Samples were dissolved in 0.06 M TrisHCl buffer, pH 6.8, containing of 6% (w/v) urea, 0.02% (w/v) EDTA, 20% (v/v) SDS and 10% (v/v) glycerol. After boiling (2 min), the samples were applied to gels and separated at 11 mA. After resolution, the gels were fixed for 1 h in 10% (w/v) sulfosalicylic acid and subsequently stained for 2 h in 0.125% (w/v) Coomassie Blue R-250 in 50% methanol and 10% acetic acid. Gel destaining was carried out first in 50% methanol and 10% acetic acid for 10 min, and then in 5% methanol and 7% acetic acid. Some gels were stained with silver according to the method of Krueger and Schwartz (*17*). To estimate the staining intensity of the individual bands, the gels were subjected to densitometric scanning on a Hoeffer Scientific densitometer. The molecular masses of intact PGs and their core proteins were calculated from the calibration curve generated by plotting the relative mobilities of standard proteins [carbonic anhydrase (29 kDa), egg albumin (45 kDa) and bovine serum albumin (67 kDa)] as well as high-molecular-weight proteins that are not yet typical mass markers [standard collagen type I, containing collagen α chains (α1 of approx. 98 kDa and α2 of approx. 90 kDa) as well as their dimers and trimers] against the log of these molecule molecular masses. Thus, the molecular masses of high-molecular-weight components present in both NF and DF extracts was evaluated only approximately.

Western Blotting—To confirm the identity of small PGs extracted from tissue samples, the immunoreactivity of these molecules was evaluated. Before that, the SDS-PAGE resolved PGs and their core proteins were electrotransferred to Immobilon P membranes in a Hoeffer semi-

dry blot module at a constant current of 40 mA for 1 h in buffer containing 0.025 M TrisHCl, 0.192 M glycine and 10% (v/v) methanol. Then, the obtained blots were incubated with chondroitinase ABC in order to remove CS/DS chains from the PGs. This step is necessary for the immunodetection of intact PGs, since GAG chains block the core protein epitopes for employed antibodies. Enzyme treatment was performed in 0.05 M TrisHCl buffer, pH 8.0, containing 1% bovine serum albumin (BSA) for 1 h at 37°C under rotation. Subsequently, blots were rinsed 3 times for 5 min each in 0.05 M TrisHCl buffer, pH 7.4, containing 0.15 M NaCl and 0.1% (v/v) Tween 20 (TBS buffer). To block non-specific antibody adsorption, the blots were incubated in TBS buffer containing 5% (w/v) Blot Quick Blocker for 1 h at 21°C. After washing with TBS (3 times, 5 min each), the membranes were treated with polyclonal rabbit anti–human decorin (LF-136) and anti–human biglycan (LF-51) antibodies. The antibodies were generously provided by Dr. L. Fisher, NIDR, Bethesda. These primary antibodies were diluted 1:500 in TBS, containing 5% (w/v) Blot Quick Blocker and incubated with blots for 1 h at 21°C. Then, membranes were washed as above and treated for 1 h at 21°C with alkaline phosphatase conjugated mouse monoclonal anti–rabbit immunoglobulin G, diluted 1:150,000 in TBS, containing 5% (w/v) Blot Quick Blocker. Immunoreactive PGs and their core proteins were visualized using a mixture of NitroBlue Tetrazolium and 5-bromo-4-chloro-3-indolyl phosphate in buffer provided by the manufacturer (Sigma, USA).

Isolation of Decorin and Biglycan Glycosaminoglycan Chains—To obtain decorin and biglycan GAG chains, the PG core proteins were exhaustively digested with papain. Proteolysis was conducted in 0.1 M phosphate buffer, pH 6.5, containing 5 mg of enzyme per 1 ml and 0.01 M cysteine HCl for 12 h at 56°C. The obtained peptides were precipitated by the addition of 100% (w/v) trichloroacetic acid (TCA) to a final concentration of 7% followed by incubation for 12 h at 4°C. The precipitate was centrifuged (7,200 × *g*, 20 min), washed with 7% TCA, and centrifuged again. The obtained pellets were discarded and the combined supernatants were treated with 5 volumes of absolute ethanol for 12 h at 4°C to precipitate GAGs/peptidoGAGs. The GAG containing pellets were collected by centrifugation (19,000 × *g*, 15 min), dried and subjected to alkaline treatment as described previously (*18*). The above procedure allows the removal of core protein fragments from peptidoGAGs. Then, the obtained samples of decorin and biglycan GAG chains were analysed for uronate content according to Blumenkrantz and Asboe-Hansen (*19*).

Analysis of Glycosaminoglycan Structure—To obtain chain regions with specific structures, *i.e.*, copolymeric sections as well as homopolymeric segments including glucuronate disaccharide clusters ("glucuronic" regions) and iduronate disaccharide clusters ("iduronic" regions), decorin and biglycan derived GAGs were digested with bovine testes hyaluronidase, chondroitinase B or chondroitinase AC I, respectively. Degradative procedures were performed as described previously (*18*). Briefly: hyaluronidase hydrolysis of GAGs was carried out in 0.1 M sodium acetate buffer, pH 5.0, containing 0.15 M NaCl, for 24 h at 37°C. Chondroitinase B degradation of GAGs was performed in 0.05 M TrisHCl buffer, pH 7.5, for 24 h at 25°C; chondroitinase AC I cleavage was conducted in 0.03 M TrisHCl buffer, pH 7.4, containing 0.03 M sodium acetate and 0.025% (w/v) BSA, for 2 h at 37°C. The GAG degradation products as well intact GAG chains were further analysed by PAGE.

Polyacrylamide Gradient Gel Electrophoresis of GAGs and Products of GAG Degradation—PAGE was carried out according to Laemmli (*16*) as modified by Lyon and Gallagher (*20*). The resolving gel consisted of a 20–25% (w/v) total acrylamide gradient with 2.5–7% (w/v) crosslinker gradient. Intact decorin and biglycan GAG chains and products of GAG degradation were resolved at 200 V after the addition of glycerol to 10% and phenol red. Electrophoresis was terminated when the phenol red reached 1.0 cm from the bottom of the gel. The gel was removed, fixed and stained, first in Azure A and then in ammoniacal silver nitrate as described by Lyon and Gallagher (*20*) and submitted to densitometry.

Statistical Analysis—Statistical analysis was carried out in order to evaluate the significance of differences in the amount of sulphated GAGs eluted at 1 M NaCl from DEAE-Sephacel in the case of Dupuytren's fascia extracts compared with normal palmar fascia extracts. Data were analysed by the Shapiro-Wilk test to verify the assumption of normal distribution. Results were expressed as mean values ± SD. Statistical evaluation was performed with the Student's *t* test, accepting $P < 0.05$ as significant.

RESULTS

Characterization of Matrix Proteoglycans from Normal Fascia and Dupuytren's Fascia—PGs extracted from separate tissue samples (Table 1) under dissociative conditions were further purified and characterized individually. The first step in glycoprotein purification was anion exchange chromatography on DEAE-Sephacel. PGs adsorbed to the bed were eluted at 1 M NaCl. The column elution patterns of sulfated GAGs (representing both PG side chains and free GAG chains) were similar for both tissues—approx. 90% of molecules were recovered at this salt concentration. However, in the case of NF the eluates contained 126 ± 42.2 μg of sulfated GAGs per 1 g dry weight, whereas the DF samples contained significantly more sulfated GAGs, *i.e.*, 282.7 ± 97 μg of per 1 g dry weight ($P < 0.05$). The components eluted at 1 M NaCl were further subjected to gel chromatography on Sepharose CL-4B. Typical elution patterns are shown in Fig. 1, a and b. As can be seen, regardless of the tissue sample, PGs fractionated into two peaks. The minor peak (peak I) comprised molecules excluded from Sepharose CL-4B. Instead, a majority of PGs eluted as a broad asymmetrical peak (peak II) with average K_{av} (K_{av} defined as a ratio of $(V_e - V_o)$ to $(V_t - V_o)$ where V_e, elution volume of molecules forming peak maximum; V_o, void volume; V_t, total volume of bed) of 0.49 and 0.40 for compounds derived from NF and DF, respectively. Species present in pooled fractions of the individual peaks (Fig. 1, a and b) were further analyzed by SDS-PAGE followed by staining with Coomassie Blue. In the case of PG samples, the material excluded from Sepharose CL-4B comprised high-molecular-weight compounds poorly penetrating into gel,

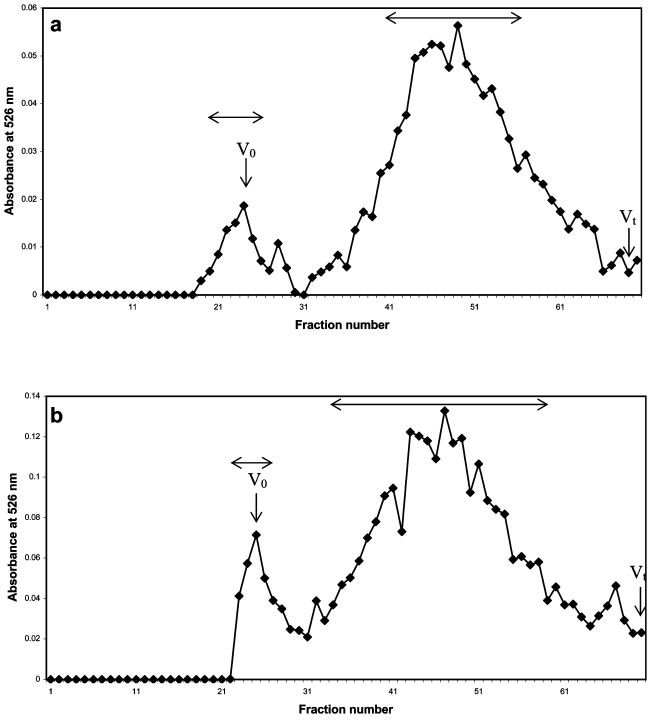

Fig. 1. **Sepharose CL-4B gel filtration of proteoglycans (PGs)/free sulfate glycosaminoglycans (GAGs) derived from a 48-year-old female with normal fascia (a) and a 49-year-old female with Dupuytren's fascia (b).** GAG material eluted from a DEAE-Sephacel ion exchange column at 1 M NaCl was subjected to gel chromatography on a Sepharose CL-4B column (1 × 44 cm) in 4 M guanidine HCl, 0.15 M sodium acetate, pH 6.3. Fractions of 0.5 ml were collected and each fraction was monitored for GAGs. Fractions containing GAGs were pooled as indicated by the bars. V_0, void volume; V_t, total volume.

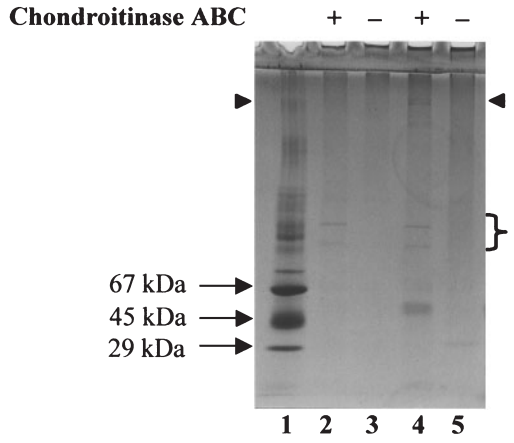

Fig. 2. **SDS-PAGE of normal fascia (NF)– and Dupuytren's fascia (DF)–derived PGs excluded from Sepharose CL-4B.** Samples of PGs and CS/DSPG core proteins obtained after chondroitinase ABC treatment were resolved in a 4–15% gradient gel, and subsequently stained with Coomassie Blue. Lane 1, molecular mass markers (carbonic anhydrase, 29 kDa; egg albumin, 45 kDa; bovine serum albumin, 67 kDa). Components of high molecular weight observed in the molecular standard lane, were formed during storage of these standards. They probably represent bovine serum albumin (BSA) oligomers formed by this cysteine-rich protein becoming linked by disulfide bonds. Such oligomers are observed when BSA is submitted to SDS-PAGE under non-reducing conditions; lane 2,chondroitinase ABC treated PG(s) derived from NF of a 55-year-old male; lane 3, intact PG(s) derived from NF of a 55-year-old male; lane 4, chondroitinase ABC treated PG(s) derived from DF of a 53-year-old male; lane 5, intact PG(s) derived from DF of a 53-year-old male. The arrowheads indicate the positions of 400 kDa and/or 450 kDa core protein bands; the bracket shows the position of chondroitinase ABC-related components.

although usually slight contamination by second peak components (showing great electrophoretic mobility) was also apparent (Fig. 2, lanes 3 and 5). Very slowly migrating species, more prominent in DF samples, particularly those derived from 46- and 49-year-old patients, were partly sensitive to chondroitinase ABC degradation. Enzyme treatment of NF-derived PGs, which was possible in the case of a few larger tissue samples, produced a barely apparent core protein band at approx. 400 kDa, as indicated by the arrowhead in Fig. 2, lane 2. Components with approx. molecular masses of 130 and 150 kDa (marked by the bracket in Fig. 2, lanes 2 and 4) are chondroitinase ABC–related. Enzyme action on peak I PGs derived from all of the DF samples resulted in the appearance of several large proteins of which those with approx. molecular masses of 400 and 450 kDa (as indicated by the arrowheads in Fig. 2, lane 4) were most prominent. The above-mentioned species were frequently contaminated with a component with an apparent molecular mass of 47 kDa, representing a small PG core protein. As opposed to the susceptibility to chondroitinase ABC, the large PG sensitivity to heparitinase action has not been proved to be due to small amounts of these glycoproteins obtained, particularly in the case of control tissue.

Regardless of the tissue sample, the components in peak II when chromatographed on Sepharose CL-4B, resolved during SDS-PAGE into two polydisperse bands (Fig. 3, lanes 3 and 4). In the case of the NF-derived PG samples the most prominent band included fast migrating species with approx. molecular masses ranging from 80 to 120 kDa (Fig. 3, lane 3). Components migrating at approx. 250 kDa formed barely stained band (marked by the arrowhead in Fig. 3, lane 3). In contrast, the bands of DF-derived small PGs showed similar staining intensities (Fig. 3, lane 4), although some differences in this respect were found for the samples from patients aged of 43, 44 and over 70 years. In the case of these specimens, rapidly moving molecules displayed approximately 1.5-fold staining intensity over that of slowly migrating species. The former components derived from DF samples had approx. molecular masses ranging from 110 to 170 kDa, while the slower species migrated at approx. 350 kDa (Fig. 3, lane 4). However, it should be noted that some differences in molecular weight of both component types derived from the various samples from NF and DF. Irrespective of tissue type, small PGs obtained from the samples from 40–50-year-old subjects displayed the highest molecular masses, while the molecular weights of the glycoproteins derived from older individuals gradually declined with age. Moreover, sex-dependent intra-group variations with regard to PG molecular masses were also found. The glycoproteins derived from females had a somewhat lower weight as compared to those from PG males of corresponding age. However, the latter data

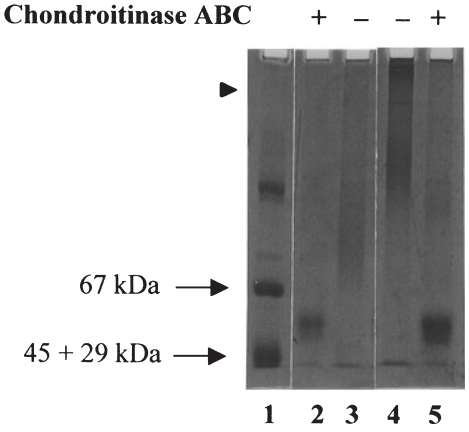

Fig. 3. **SDS-PAGE of normal fascia (NF)– and Dupuytren's fascia (DF)–derived PGs eluted from Sepharose CL-4B as peak II.** Samples of PGs and chondroitin sulfate/dermatan sulfate proteoglycan (CS/DSPG) core proteins obtained after chondroitinase ABC treatment were resolved in a 7% gel, and subsequently stained with Coomassie Blue. Lane 1, molecular mass markers (carbonic anhydrase, 29 kDa; egg albumin, 45 kDa; bovine serum albumin, 67 kDa); lane 2, chondroitinase ABC treated PG(s) derived from NF of a 55-year-old male; lane 3, intact PG(s) derived from NF of a 55-year-old male (the arrowhead indicates the position of the 250 kDa component band); lane 4, intact PG(s) derived from DF of a 54-year-old male, lane 5, chondroitinase ABC treated PG(s) derived from DF of a 54-year-old male.

need to be confirmed due to the small number of samples compared. Nevertheless, irrespective of small PG mass alterations observed within each group of tissue samples, the macromolecules isolated from the palmar fascia of Dupuytren's patients always displayed significantly higher molecular weights than those of the glycoproteins derived from healthy individuals of corresponding age. On the other hand, to eliminate (or at least to limit) the impact of non-Dupuytren's disease connected factors on PG metabolism, the macromolecules derived from healthy subjects and patients of corresponding sex and age were compared.

Both small PGs present in all of the NF and DF samples were completely resistant to heparitinase (data not shown) and sensitive to chondroitinase ABC. Electrophoregrams of the latter enzyme–treated samples lacked the above-mentioned diffuse bands (Fig. 3, lanes 3 and 4 *versus* Fig. 3, lanes 2 and 5), whereas the appearance of a closely spaced core protein doublet was found (Fig. 3, lanes 2 and 5). The proteins demonstrated apparent molecular masses of 47 and 49 kDa in all of the NF and DF samples.

In spite of the absence of differences in small PG core protein electrophoretic mobility when NF and DF samples were compared, significant alterations in core protein staining intensity were observed. In all of the NF samples, faster migrating small PG core proteins were less visible (Fig. 3, lane 2), while bands of DF-derived core proteins showed almost similar staining (Fig. 3, lane 5).

Two small PGs found in NF and DF extracts represent decorin and biglycan as judged from the molecular masses of the intact molecules and core proteins, as well as the types of GAG side chains. To confirm this suggestion, PG immunoreactivity was evaluated. The analysis was carried out for core proteins derived from two samples each of NF and DF small PGs (NF from a 54-year-old female and a 55-year-old male; DF from a 54-year-old female and a 54-year-old male). Single PG samples (from a 55-year-old healthy male and a 54-year-old male with Dupuytren's disease) were used to evaluate intact glycoprotein immunoreactivity. The selected samples were representative of both groups.

Antiserum against a peptide near the N-terminus of decorin (LF-136) identified as the decorin core protein the component migrating at 49 kDa in both NF extracts, as can be seen in a typical blot (Fig. 4a, lane 3). On the other hand, two proteins with molecular masses of 47

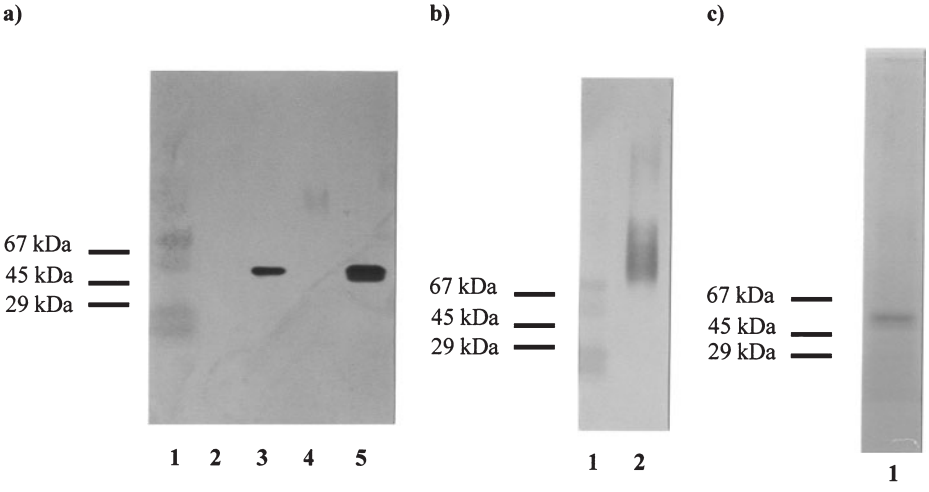

Fig. 4. **(a) Polyacrylamide gel blots of normal fascia (NF)– and Dupuytren's fascia (DF)–derived small PGs probed with antiserum against human decorin (LF-136).** PGs and their core proteins were first resolved in a 4–15% gradient gels, electrotransferred to Immobilon P, and then immunostained by LF-136. The migration positions of the molecular weight standards are as indicated. Lane 1, electrotransfer markers; lane 2, 55-year-old male NF-derived decorin; lane 3, 55-year-old male NF-derived decorin core protein; lane 4, 54-year-old male DF-derived decorin; lane 5, 54-year-old male DF-derived decorin core proteins. **(b) Immunoreactivity of small PGs present in combined NF extracts (derived from a 55-year-old male and a 54-year-old female) with antiserum against human decorin (LF-136).** PGs were first resolved in a 4–15% gradient gels, electrotransferred to Immobilon P, and then probed with LF-136. Lane 1, electrotransfer markers; lane 2, decorin present in combined extracts of two NF samples. The migration positions of the molecular weight standards are as indicated. **(c) SDS-PAGE of a 55-year-old male NF-derived decorin core protein variants.** The core proteins obtained after chondroitinase ABC treatment of purified decorin were resolved in a 4–15% gradient gel and then stained with Coomasie Blue (lane 1). The migration positions of the molecular weight standards are as indicated.

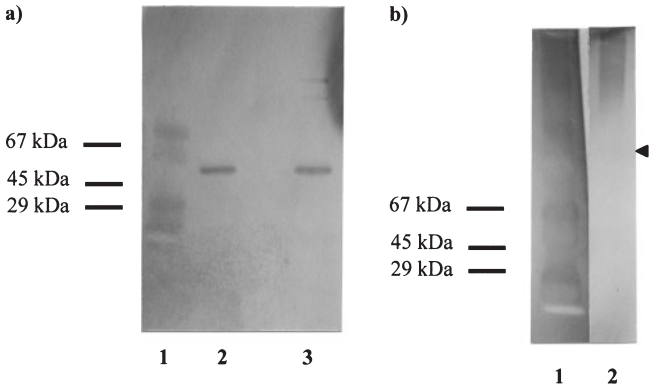

Fig. 5. **Polyacrylamide gel blots of normal fascia (NF)– and Dupuytren's fascia (DF)–derived small PGs probed with antiserum against human biglycan (LF-51).** PG core proteins (a) and DF-derived PGs (b) were first resolved in a 4–15% gradient gels, electrotransferred to Immobilon P, and then immunostained by LF-51. The migration positions of the molecular weight standards are as indicated. (a) Lane 1, electrotransfer markers; lane 2, a 55-year-old male NF-derived biglycan core protein; lane 3, a 54-year-old male DF-derived biglycan core proteins. (b) Lane 1, electrotransfer markers; lane 2, a 54-year-old male DF-derived biglycan. The arrowhead indicates the migration position of components moving as decorin.

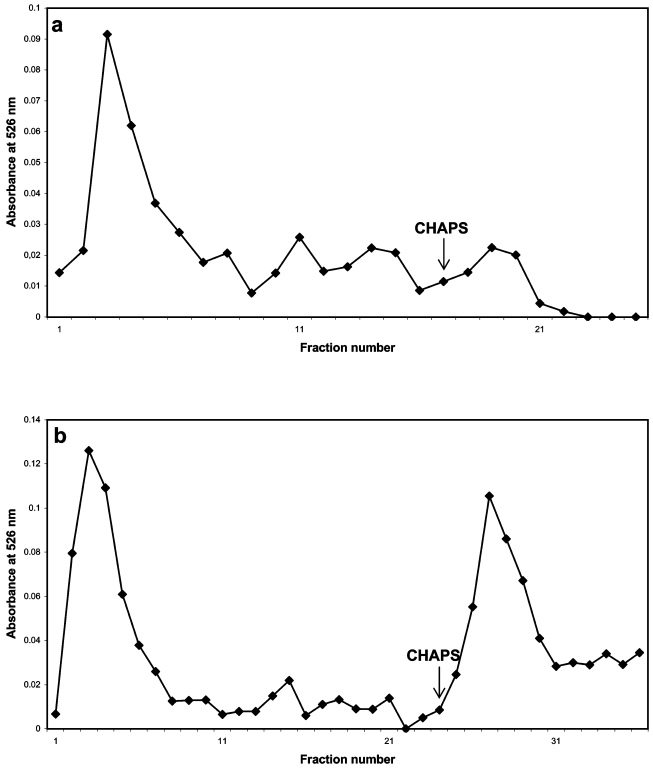

Fig. 6. **Hydrophobic interaction chromatography of small PGs derived from normal fascia of a 58-year-old female (a) and Dupuytren's fascia of a 54-year-old female (b).** Small PGs were separated on an octyl-Sepharose CL-4B column equilibrated in 4 M guanidine HCl (GdnHCl), 0.15 M sodium acetate, pH 6.3. Unbound PG material was eluted in equilibrating buffer; PG(s) bound to the bed were eluted with 1% CHAPS in 4 M GdnHCl. The arrow indicates the appearance of CHAPS in the eluates. Eluate fractions were assayed for total glycosaminoglycans by reaction with dimethylmethylene blue dye.

and 49 kDa in the DF-derived samples demonstrated immunoreactivity with LF-136 (Fig. 4a, lane 5). The lack of 47 kDa core protein immunostaining by LF-136 on NF-derived small PG blots may be due to the small amount of this component in samples subjected to Western blotting (and in tissue extracts). This suggestion is supported by the results of SDS-PAGE carried out on purified decorin core protein variants derived from one NF sample probed with LF-136 (Fig. 4c, lane 1). Moreover, similar electrophoretic patterns of decorin core proteins were found for all of the other three NF samples (from a 48-year-old female, a 64-year-old female and a 69-year-old male). Nevertheless, other explanations for the phenomenon visible on NF-derived PG core protein immunoblots probed with LF-136 cannot be excluded. It is conceivable that the 47 kDa core protein of NF-derived decorin lacks epitopes recognized by LF-136 due to mRNA alternative splicing. Moreover, the presence of a new CS/DSPG co-fractionating with NF decorin and characterized by its 47 kDa core protein should be considered. However, these hypotheses seem unlikely in light of the present knowledge. Similarly, a hypothesis for epitope masking due to changes in decorin core protein conformation seems to be nearly impossible.

The immunologic identification of intact fascia PGs with LF-136 indicates that material moving as a diffuse band at approx. 110–170 kDa on DF-derived small PG blot represents decorin (Fig. 4a, lane 4). On the other hand, the lack of PG immunostaining in the case of the NF sample (Fig. 4a, lane 2) is probably due to the small amount of protein used for Western blotting. This suggestion results from the fact that in a sample combining two NF specimen extracts (from a 55-year-old male and a 54-year-old female) at a ratio of 1:1, the presence of 80–120 kDa PG demonstrating LF-136 immunoreactivity was found (Fig. 4b, lane 2). Moreover, LF-136 immunoreactivity in this sample was also observed for components migrating at approx. 250 kDa (Fig. 4b, lane 2). Similar species probably representing decorin that cross-linked to other matrix molecules were also found in skin extracts (*21*).

Antibodies to a peptide near the N-terminus of biglycan (LF-51) immunostained the 47 kDa core protein in NF-derived PG samples, and the 47, 170 and 240 kDa core proteins in the case of DF samples as shown on typical blots (Fig. 5a, lanes 2 and 3). The presence on the DF sample blots of high-molecular-weight species showing reactivity with LF-51 indicates that biglycan can cross-link to other molecules in the DF matrix. It should be noted that similar biglycan-related components with high molecular weights were observed in skin extracts (*21*).

In the case of DF sample, immunostaining by LF-51 was also found for PG with molecular masses of approx. 350 kDa (Fig. 5b, lane 2). However, few molecules migrating as DF decorin (indicated by the arrowhead in Fig. 5b, lane 2) showed this immunoreactivity as well. On the other hand, the NF intact biglycan was not subjected to immunostaining due to its very low content in tissue extracts (for immunostaining intact PG, at least 3 times more protein is needed than when the immunoreactivity of the core protein is studied). However, it can be pre-

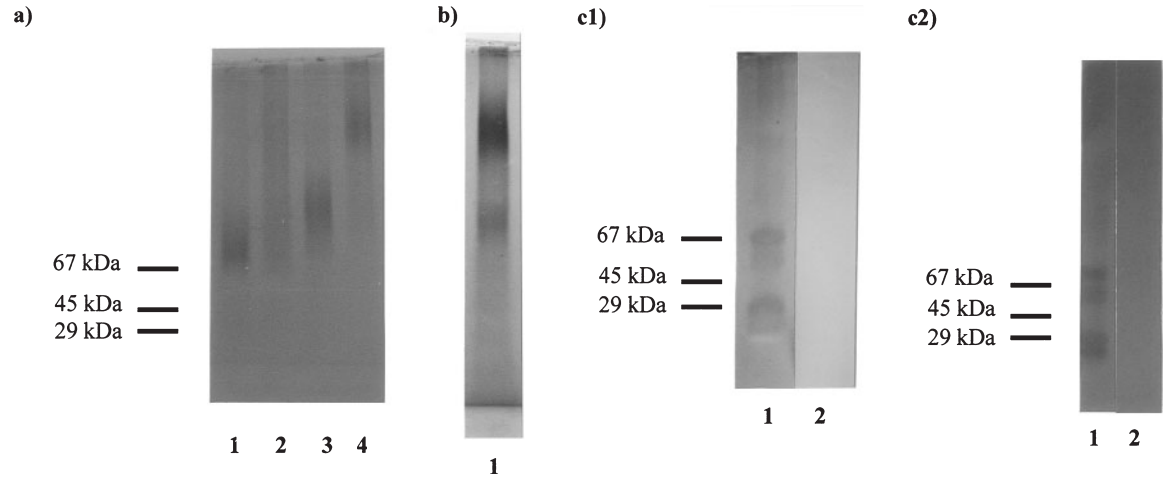

Fig. 7. **(a) SDS-PAGE of PG material not bound to octyl-Sepharose CL-4B in the presence of 4 M guanidine HCl (GdnHCl), or eluted from the bed with 1% CHAPS in 4 M GdnHCl.** Samples of small PGs derived from both normal fascia (NF) and Dupuytren's fascia (DF) were resolved in a 4–15% gradient gels and stained with Coomasie Blue. The migration positions of the molecular weight standards are as indicated. Lane 1, unbound PG derived from NF of a 48-year-old female; lane 2, a 48-year-old female NF-derived PG(s) eluted from octyl-Sepharose with 1% CHAPS; lane 3, unbound PG derived from DF of a 49-year-old female; lane 4, a 49-year-old female DF-derived PG(s) eluted from octyl-Sepharose with 1% CHAPS. **(b) SDS-PAGE of a 54-year-old female NF-derived PG(s) that bound to octyl-Sepharose at 4 M GdnHCl after re-chromatography on the same bed in the presence of 2 M GdnHCl and elution at high GdnHCl concentration (lane 1).** (c_1) Reactivity of core protein(s) of a 56-year-old male DF-derived PG not bound to octyl-Sepharose CL-4B at 4 M GdnHCl, with antiserum to human biglycan (LF-51). Lane 1, electrotransfer markers; lane 2, core protein(s) probed with LF-51. (c_2) Reactivity of core protein(s) of a 56-year-old male DF-derived PG adsorbing to octyl-Sepharose CL-4B at 4 M GdnHCl, with antiserum to human decorin (LF-136). Lane 1, electrotransfer markers; lane 2, core protein(s) probed with LF-136.

sumed that in the case of NF extracts, biglycan is represented at least by species migrating in SDS-PAGE at approx. 250 kDa as judged from the known ability of PG to self- associate in 0.375 M Tris HCl (used in the Laemmli electrophoretic system) leading to a decrease in glycoprotein electrophoretic mobility in comparison to that of decorin (*22*).

To separate biglycan from decorin, samples of NF- and DF-derived small PGs were submitted to hydrophobic interaction chromatography on octyl-Sepharose CL-4B in 4 M GdnHCl. In all PG samples, two fractions were obtained, as can be seen from typical chromatogram patterns (Fig. 6, a and b). The first fraction contained material that did not bind to octyl-Sepharose, and the second comprised PG(s) bound to the bed and eluted by 1% CHAPS. The particularly abundant fraction of unbound PG(s) and the small fraction of bound material were found in all NF-derived samples (Fig. 6a), whereas in a majority of the DF samples, PG material was almost equally divided into the two above-mentioned fractions (Fig. 6b). Only in samples from the 43, 44 and above 70-year-old patients was the fraction of PG(s) adsorbing to the bed clearly smaller (data not shown). To characterize the obtained PG fractions, their components were subjected to SDS-PAGE. The electrophoregrams indicate that regardless of the tissue sample, unbound material contained only molecules moving as decorin (Fig. 7a, lanes 1 and 3), while the fraction eluted with 1% CHAPS included biglycan (Fig. 7a, lanes 2 and 4). However, each fraction of PG(s) adsorbing to bed also contained components migrating as decorin (Fig. 7a, lanes 2 and 4). To verify the purity of all PG fractions, the molecules were submitted to re-chromatography on octyl-Sepharose CL-4B at 2 M GdnHCl and then eluted with a linear gradient of 2–6 M GdnHCl. In the case of both palmar fascia types (*i.e.* NF and DF), the species comprising the material not bound to the bed at 4 M GdnHCl, when chromatographed in the presence of 2 M GdnHCl, eluted as a single peak at low GdnHCl concentration (data not shown). Instead, DF-derived PG(s) that adsorbed to octyl-Sepharose at 4 M GdnHCl, also eluted as a single peak, but at high GdnHCl concentration when chromatographed at 2 M GdnHCl (data not shown). In the case of the NF samples, the PGs binding to the bed at 4 M GdnHCl separated into two molecular fractions when re-chromatographed at 2 M GdnHCl (data not shown). The minor fraction comprised molecules eluted at low GdnHCl concentration, while the major fraction contained species desorbed from the bed at high GdnHCl concentration. It seems that decorin contamination of the biglycan fraction obtained after hydrophobic interaction chromatography of NF samples at 4 M GdnHCl can result from technical problems with the preservation of the proper ratio of small PG amount to bed volume due to the small amounts of these molecules. To resolve this problem, chromatography at 2 M GdnHCl was carried out in thin calibrated tubes.

The NF-derived molecules adsorbed more avidly to octyl-Sepharose at 2 M GdnHCl displayed homogeneity when again subjected to hydrophobic interaction chromatography under the same conditions (data not shown). However, during SDS-PAGE the species still separated into two bands as shown in Fig. 7b, lane 1, which shows the electrophoretic pattern of a 54-year-old female PG. Moreover, similar results were obtained for two other PG samples (from a 48-year-old female and a 69-year-old male; data not shown). It seems that components moving as decorin can represent biglycan with distinct polysaccharide substitutions. Such species present in DF sam-

ples displayed immunoreactivity with antiserum against recombinant biglycan (Fig. 5b, lane 2). To confirm the purity of the PG fractions obtained after hydrophobic interaction chromatography on octyl-Sepharose CL-4B in 4M GdnHCl, Western blotting was also performed. However, the latter procedure was employed only in the case of a few samples of DF-derived PGs due to insufficient amounts of material. Both DF decorin and DF biglycan did not display any cross-immunoreactivity with anti–human biglycan (LF-51) or anti–human decorin (LF-136) antibodies, as judged from typical blots (Fig. 7, c_1 and c_2).

Evaluation of NF- and DF-Derived Small PG Glycosaminoglycan Structure—To evaluate glycosaminoglycan chain molecular masses and composition, GAGs released from individual small PG samples after core protein proteolysis by papain followed by alkaline elimination were submitted to PAGE, before and after treatment with various enzymes. The following enzymes were used: testicular hyaluronidase, chondroitinase AC I and chondroitinase B. Testicular hyaluronidase hydrolyzes (β1→4) linkages between GalNAc and GlcA residues (*23*). However, the enzyme requires at least two GlcA repeat disaccharide sequences (*23*). Thus, hyaluronidase depolimerizes chondroitin-4-sulfate (C-4-S) and chondroitin-6-sulfate (C-6-S) to okta- but mainly to tetra- and hexasaccharides, while the enzyme action on DS yields a series of oligosaccharides with the general structure GlcA-GalNAc-(IdoA/GlcA-GalNAc)$_n$-GlcA-GalNAc, where n is the number of disaccharide repeats resistant to degradation (*23*). Hyaluronidase treatment of NF- and DF-derived PG glycosaminoglycans should identify copolymeric regions and/or homopolimeric segments (*i.e.* clusters of disaccharide repeats with iduronate residue and clusters maximally of four disaccharide repeats with glucuronate residue) if present in GAG chains. To reveal the presence of iduronate disaccharide clusters ("iduronic" regions) in small PG glycosaminoglycan chains, GAG sensitivity to chondroitinase AC I was assessed as the enzyme cleaves only (β1→4) links between GalNAc and GlcA residues (*24*). Then, among the products of DS and CS degradation by chondroitinase AC I, ΔHexA-(GalNAc-IdoA)$_n$-GalNAc and/or ΔHexA-GalNAc are found, in which n is the number of disaccharide repeats resistant to degradation and ΔHexA represents 4-deoxy-L-threo-hex-4-enopyranosyluronic acid (*24*).

Apart from copolymeric and "iduronic" segments, the contribution of glucuronate disaccharide clusters ("glucuronic" regions) to the composition of NF- and DF-derived small PG glycosaminoglycans was also evaluated. The latter chain fragments were obtained after chondroitinase B action as the lyase splits GalNAc- IdoA links in DS chains to generate degradation products that include ΔHexA-GalNAc and ΔHexA-(GalNAc-GlcA)$_n$-GalNAc (*24*). However, it should be emphasized that among all products received after single enzyme action on GAGs, di- and tetrasaccharides are undetectable by Azure A/ammoniacal silver staining after PAGE due to their unsuitable charge (*20*). Nevertheless, simultaneous analysis of products obtained after independent action of three enzymes (chondroitinase AC I, chondroitinase B and testicular hyaluronidase) on the same GAG material avoids this limitation and yields almost complete data about GAG composition. For example, chondroitinase AC I depolymerizes DS chain segments consisted of glucuronate disaccharide clusters mainly to disaccharides. However, simultaneously conducted degradation of the same GAG material by chondroitinase B (enzyme with complementary degradation properties that acts on DS) allows detection of all of such chain regions (*20*). Similarly, "iduronic" regions degraded by chondroitinase B to disaccharides can be shown after action of chondroitinase AC I. Moreover, DS cleavage by hyaluronidase, which does not degrade chain segments comprising single glucuronate disaccharides flanked by iduronate disaccharide clusters or single glucuronate disaccharides alternating with single iduronate disaccharides, allows additionally the visualization of these fragments depolymerized by chondroitinase B and/or AC I to saccharides undetectable by Azure A (*20*, *23*).

To evaluate the relationship between the molecular size of the GAG degradation products and their electrophoretic mobility in the gradient gel [20–25% (w/v) total acrylamide gradient with a 2.5–7% (w/v) crosslinker gradient], saccharides obtained after partial depolymerization of standard C-4-S and standard DS by chondroitinase AC I were first separated by chromatography on Bio-Gel P-10 and then electrophoresed in the same gels. The results (data not shown) indicated that the above gradient gel separated GAG derived oligosaccharides principally on the basis of molecular size.

NF and DF Biglycan GAG Structure—Regardless of the tissue source, the biglycan GAG chains showed remarkable molecular mass heterogeneity, migrating in PAGE as broad, polydisperse bands (Fig. 8a, lanes 2 and 3). Moreover, GAGs derived from all of the biglycan samples irrespective of tissue type, had apparent molecular masses ranging from several hundred Da to 14 kDa as compared with simultaneously electrophoresed reference DS with molecular masses of 11–25 kDa (Fig. 8a, lane 1). However, it should be noted that within NF biglycan GAG chains, those with smaller molecular masses prevailed, while in the case of DF biglycan, the amounts of high and small molecular mass chains were almost equal (Fig. 8a, lanes 2 and 3). However, individual intra-group differences in biglycan GAG molecular size were difficult to assessment due to poor staining of intact chains by ammoniacal silver (*20*). Simultaneously, this sensitive staining method had to be used because of the small amounts of GAGs. Nevertheless, it may be presumed that irrespective of fascia type, age-related alterations in PG GAG chain molecular size resembling those found for intact glycoprotein weight occur. This results from the fact that biglycan molecules derived from all tissue samples had core proteins with the same molecular mass.

Commonly, GAG chains derived both from NF and DF biglycan samples displayed little if any sensitivity to hyaluronidase, as seen in comparisons of the degradation product electrophoretic patterns with those of intact glycosaminoglycans (Fig. 8b, lanes 1 and 2 *versus* Fig. 8a, lanes 2 and 3). On the other hand, standard C-4-S treated with hyaluronidase under the same conditions was almost completely degraded (Fig. 8b, lane 3 *versus* lane 4). The data suggest that NF and DF biglycans bear DS chains with high contents of iduronate disaccharides. This hypothesis was further verified by evaluating biglycan GAG sensitivity to chondroitinase AC I and B. How-

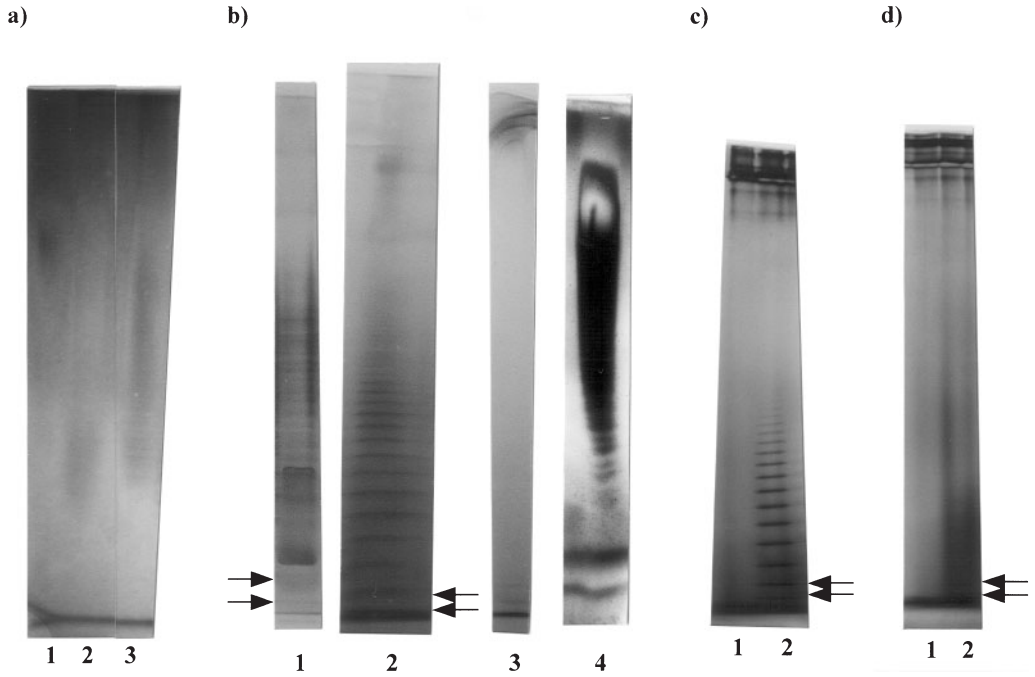

Fig. 8. **PAGE of biglycan DS chains (a) and products of their degradation by testicular hyaluronidase (b), chondroitinase AC I (c) and chondroitinase B (d).** Samples were electrophoresed in a 20–25% gradient gels containing of 2.5–7% crosslinker gradient, and then stained with Azure A/ammoniacal silver. (a) Lane 1, standard DS of molecular masses 11–25 kDa; lane 2, intact DS chains (1 μg of hexuronic acids) derived from a 58-year-old female normal fascia (NF) biglycan; lane 3, intact DS chains (1 μg of hexuronic acids) derived from a 54-year-old female Dupuytren's fascia (DF) biglycan. (b) Lane 1, a 54-year-old female NF biglycan DS (1 μg of hexuronic acids) depolymerized by hyaluronidase; lane 2, a 54-year-old female DF biglycan DS (1 μg of hexuronic acids) depolymerized by hyaluronidase; lane 3, standard C-4-S after hyaluronidase action; lane 4, standard C-4-S before hyaluronidase treatment. (c) Lane 1, chondroitinase AC I; lane 2, a 53-year-old male DF biglycan DS (1 μg of hexuronic acids) after degradation by chondroitinase AC I. (d) Lane 1, chondroitinase B; lane 2, a 53-year-old male DF biglycan DS (1.5 μg of hexuronic acids) after action of chondroitinase B. The arrows show migration positions of saccharides obtained by complete depolymerization of standard chondroitin-4-sulfate from whale cartilage by testicular hyaluronidase.

ever, in these studies, only DF biglycan GAG samples were used due to the very small amounts of DS chains obtained from NF-derived biglycan samples as a consequence small content of this PG in normal tissue.

DS from DF biglycan samples also demonstrated significant resistance to chondroitinase AC I as can be seen from a typical electrophoretic pattern of the degradation products of this GAG (Fig. 8c, lane 2). However, among the degradation products, an increase in the contents of species with smaller molecular masses and the disappearance of some high-molecular-mass components were observed as compared with hyaluronidase resistant saccharides (Fig. 8c, lane 2 *versus* Fig. 8b, lane 2). Nevertheless, the above results unequivocally indicate that at least DF biglycan DS chains contain mainly iduronate disaccharide clusters. These "iduronic" segments are separated by/associated with rather short clusters of glucuronate disaccharides as judged from the observation that DS fragments resistant to chondroitinase B show high electrophoretic mobility (Fig. 8d, lane 2). Moreover, it is not unlikely that some of the latter saccharides include a tetrasaccharide linkage region adjacent to a "glucuronic" segment as such chain sections are resistant to lyase (*24*).

Quantitative analysis of DF biglycan DS degradation products detected on the electrophoregrams revealed that the contribution of glucuronate disaccharide clusters to GAG chain composition is insignificant when compared to the content of "iduronic" sections (data not shown). It can be postulated, therefore, that part of the latter regions are separated by/associated with single glucuronate disaccharides forming in DS chains long copolymeric segments resistant to hyaluronidase (Fig. 8b, lane 2) and sensitive to chondroitinase AC I (Fig. 8c, lane 2).

Structure of NF and DF Decorin GAGs—Regardless of tissue sample, the majority of decorin GAG chains displayed higher molecular masses than biglycan dermatan sulfates (Fig. 9a$_1$, lane 1 and Fig. 9a$_2$, lane 2 *versus* Fig. 8a, lanes 2 and 3). Intact GAG chains of NF decorin samples had apparent molecular masses ranging from 5 to 22 kDa (Fig. 9a$_1$, lanes 1 and 2), whereas GAG chains derived from DF decorin samples showed molecular masses between 11 and 24 kDa (Fig. 9a$_2$, lanes 1 and 2) as compared to simultaneously elecrophoresed standard DS with molecular masses of 11–25 kDa. However, individual intra-group deviations with respect of decorin GAG chain molecular size were difficult to assess for the same reason as in the case of biglycan DS. Nevertheless, it seems, that decorin GAG chain weight undergoes age-related alterations resembling those suggested for biglycan DS.

The electrophoretic patterns of products obtained after hyaluronidase action on GAGs from both NF and DF decorin samples were ladder-like with similar designs of

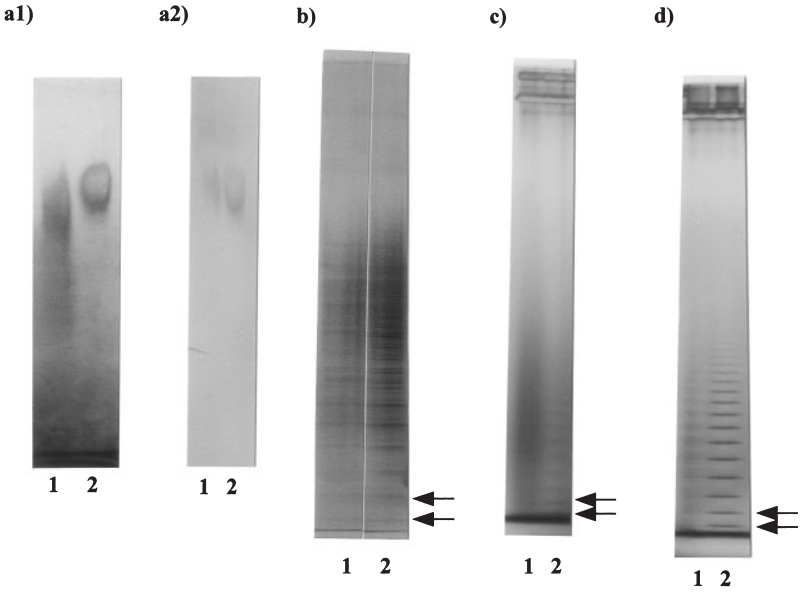

Fig. 9. **PAGE of decorin DS chains (a_1 and a_2) and products of their degradation by testicular hyaluronidase (b), chondroitinase B (c) and chondroitinase AC I (d).** Samples were electrophoresed in 20–25% gradient gels containing of 2.5–7% crosslinker gradient, and then stained with Azure A/ammoniacal silver. (a_1) Lane 1, intact DS chains (1 μg of hexuronic acids) derived from a 48-year-old female normal fascia (NF) decorin; lane 2, standard DS of molecular masses 11–25 kDa. (a_2) lane 1, standard DS; lane 2, intact DS chains (1 μg of hexuronic acids) derived from a 49-year-old female Dupuytren's fascia (DF) decorin. (b) Lane 1, a 55-year-old male NF decorin DS (1 μg of hexuronic acids) depolymerized by hyaluronidase; lane 2, a 56-year-old male DF decorin DS (1 μg of hexuronic acids) degraded by hyaluronidase. (c) Lane 1, a 48-year-old female NF decorin DS (1.5 μg of hexuronic acids) after action of chondroitinase B; lane 2, a 49-year-old female DF decorin DS (1.5 μg of hexuronic acids) after degradation by chondroitinase B. (d) Lane 1, a 48-year-old female NF decorin DS (1 μg of hexuronic acids) depolymerized by chondroitinase AC I; lane 2, a 48-year-old female DF decorin DS (1 μg of hexuronic acids) after action of chondroitinase AC I. The arrows show migration positions of saccharides obtained by complete depolymerization of standard chondroitin-4-sulfate from whale cartilage by testicular hyaluronidase.

distinctly apparent main bands with interspersed weakly visible bands (Fig. 9b, lanes 1 and 2). However, in the case of DF decorin GAG degradation products with intermediate and high mobility, an increased proportion of components forming main bands to those in interspersed bands was found (Fig. 9b, lanes 1 and 2). Simultaneously, individual intra-group differences in the electrophoretic patterns were poorly manifested and frequently limited to an increased content of single saccharides. Nevertheless, it can be concluded that regardless of tissue type, decorin GAG chains derived from 40–49-year-old individuals contain somewhat more of both short and very long regions resistant to hyaluronidase as compared with glycans derived from older subjects. On the other hand, GAG chains from all decorin samples, regardless of tissue type, manifested higher sensitivity to hyaluronidase than biglycan DS when the electrophoretic patterns of degradation products were compared to those of intact glycan chains (Fig. 9b *versus* Fig. 9a_1, lane 1 and Fig. a_2, lane 2 as well as Fig. 8b, lanes 1 and 2 *versus* 8a, lanes 2 and 3). Simultaneously, decorin GAGs still showed remarkably higher resistance to enzymatic hydrolysis than standard C-4-S (Fig. 9b, lanes 1 and 2 *versus* Fig. 8b, lane 3). These data suggest that NF and DF decorins bear DS chains with a higher proportion of glucuronate residues compared to iduronate residues than biglycan GAGs. This suggestion is supported by the observation that in DS chains derived from both NF and DF decorin samples, the contents of chondroitinase B–resistant segments able to be detected by staining are enhanced, as can be seen from typical electrophoretic patterns of these GAG degradation products (Fig. 9c, lanes 1 and 2 *versus* Fig. 8d, lane 2). Nevertheless, some differences were found between NF and DF decorin DS with regard to the contents of particular "glucuronic" segments when electrophoregrams of degradation products obtained after chondroitinase B action were compared (Fig. 9c, lanes 1 and 2). In the case of NF decorin samples, the DS chains showed enhanced amounts of slower migrating saccharides resistant to the enzyme, while GAG chains of DF decorin samples manifested higher contents of very fast migrating species (Fig. 9c, lanes 1 and 2). Intra-group differences in the contribution of "glucuronic" segments in decorin DS structure were poorly marked. It seems however, that irrespective of fascia type, the amount of longer "glucuronic" regions increases somewhat in the PG GAG chains during the course of aging.

Despite a relatively high number of "glucuronic" segments, DS chains from all decorin samples still displayed a significant content of "iduronic" regions as judged from the high resistance of these GAGs to chondroitinase AC I (Fig. 9d, lanes 1 and 2). Nevertheless, among products obtained after lyase action on both tissue decorin dermatan sulfates, an increase in the amounts of compounds with high electrophoretic mobility was always observed as compared to the electrophoretic patterns of hyaluronidase-resistant chain fragments (Fig. 9d, lanes 1 and 2 *versus* Fig. 9b, lanes 1 and 2). However, "iduronic" regions of DF decorin DS most frequently demonstrated lower heterogeneities than those of segments derived from NF decorin GAG as judged from the electrophoretic patterns of saccharides resistant to chondroitinase AC I (Fig. 9d, lanes 1 and 2). In the case of the latter PG, the presence of few more weakly stained bands interspersed between bands of major species was revealed (Fig. 9d, lane 1). In contrast, electroforegrams of DF decorin DS degradation products showed bands of major components usually accompanied by only single slower moving compounds (Fig. 9d, lane 2). The observed phenomenon can result from differences in the sulfation degree of "iduronic" sections (*20*). Apart from the presence of oversulfated "iduronic" regions, DF decorin DS seems to have a greater number of iduronate disaccharide clusters per GAG chain than this glycan derived from normal tissue PG. This conclusion is based on the following findings. First, a high proportion of DF decorin DS chains had higher

molecular masses (and, at least in some cases, longer lengths) than NF decorin GAG chains (Fig. 9a$_2$, lane 2 and Fig. 9a$_1$, lane 1). Then, GAG material taken in equal amounts for chondroitinase AC I degradation comprised a smaller number of DF decorin DS chains than NF decorin GAG chains. Simultaneously, similar contents of lyase resistant saccharides were obtained in the case of both types of DS as estimated on the basis of the area under the densitometric scans (data not shown). Secondly, quantitative analysis of detectable products obtained after chondroitinase B and AC I action on decorin dermatan sulfates indicated that DF decorin GAG chains contain a higher proportion of "iduronic" sections to "glucuronic" sections (Fig. 9d, lane 2 *versus* Fig. 9c, lane 2) than NF decorin DS (Fig. 9d, lane 1 *versus* Fig. 9c, lane 1). Moreover, this finding suggests that, in the former GAG chains, greater part of "iduronic" sections is separated by single glucuronate disaccharides.

DISCUSSION

Our study was undertaken to evaluate the matrix PGs in NF and DF. The data obtained indicate that these tissues are characterized by different PG compositions. The PG profile of NF resembles that observed for fascia lata (*15*), medial collateral ligament (*25*) and skin (*21*). In these tissues, decorin (DSPG representing the family of small leucine-rich PGs) is the most abundant matrix PG, while biglycan, another member of this family along with versican, large CS/DSPG binding hyaluronic acid, exist as minor components. In the present study we focused on an extensive characterization of palmar fascia small PGs. Our findings show that the NF decorin core protein displays some heterogeneity with regard to molecular mass. The higher molecular mass form of the decorin core protein is predominant. The observed differences may result from divergence in *N*-linked oligosaccharide substitutions in the decorin core protein (*26*). The other glycan components of NF decorin molecules, DS chains, demonstrated a distinct structure from that found for normal tissue biglycan GAG. The former GAG chains have larger molecular masses and a different pattern of C-5-uronosyl epimerisation as judged from their enhanced sensitivity to hyaluronidase degradation. The presence of structural differences between decorin and biglycan dermatan sulfates confirms the key role of the PG core protein in GAG side chain modifications probably affecting the regulation of the transport of synthesized molecules into particular subcellular compartments (*27*, *28*). However, on the other hand, our findings also indicate that the NF biglycan core protein, which shows homogeneity when electrophoresed in the presence of SDS and then immunostained or detected with Coomassie Blue, can exist with different modes of GAG substitution resulting in the appearance of two PG variants. The predominant biglycan isoform has a high molecular mass, while the considerably less abundant variant has a molecular mass similar to that of decorin. The mechanism for this phenomenon remains unclear. In contrast, biglycan isoforms synthesized by human lung fibroblasts demonstrated differences in both GAG substitution and core protein mass/composition (*29*). It cannot be excluded that similar alterations in biglycan core proteins occur in the case of NF-derived PG. However, these changes are undetectable due to the very small content of the biglycan smaller variant in palmar fascia.

Dupuytren's disease is associated with significant alterations in the palmar fascia matrix PG profile as judged from tissue extract analysis. The most prominent change is the accumulation of a high-molecular-weight biglycan isoform that additionally shows an increase in the molecular masses of some of its DS chains. Moreover, an enhanced amount of CS/DS chain bearing large matrix components is also apparent in DF. In contrast to NF- derived large PG, which has a core protein with a molecular mass corresponding to that of the core protein of versican splice variant V1 (*30*), DF-derived molecules exhibited the presence of few core proteins. It seems that some of these latter components may represent the biglycan core protein cross-linked to various matrix molecules as judged from immunologic identification. However, an increased expression of versican splice variants should also be considered as occurring in DF and resulting in the appearance of the above-mentioned high-molecular-weight protein compounds.

Our data suggest that the decorin content in Dupuytren's fascia is not significantly altered as compared with normal tissue. This conclusion is based on the following. Decorin and biglycan usually bear one and two GAG side chains, respectively. Simultaneously, DF-derived decorin DS chains showed an average molecular mass approximately twice that of DF biglycan GAGs. Moreover, the biglycan content in disease affected tissue samples frequently corresponded to that of decorin, while the former PG was present in NF in negligible amounts as judged from the electrophoregrams stained with Coomassie Blue. Therefore, the alteration in biglycan content (together with enhanced amounts of CS/DS containing large components) found in DF accounts for most of the above twofold increase in the amount of sulfated GAGs extracted from disease affected tissue as compared to NF. However, despite few, if any, quantitative changes, DF-derived decorin undergoes several qualitative alterations. The majority of them are associated with the remodeling of decorin DS chains. At least a portion of these chains have higher molecular masses and/or different sulfation and C-5-uronosyl epimerisation patterns as compared with NF decorin GAG chains. However, DF decorin DS still displays a chain structure distinct from that of DF biglycan GAG. Interestingly, the appearance of DF decorin DS chains with altered structures is accompanied with an increase in the amount of core protein, probably substituted with minor numbers of *N*-linked oligosaccharides. The relationship between the above phenomena requires further investigation. Nevertheless, it is known that *N*-glycosylation influences protein folding or conformation as well as binding affinity for various ligands (*31*). Therefore, the protein *N*-glycosylation pattern could regulate the molecular attachment to the inner membrane surface of the endoplasmic reticulum and Golgi apparatus. This interaction seems to be pivotal for PG intracellular trafficking and biosynthesis (*32*). Thus, a different mode of DF decorin core *N*-glycosylation may lead to changes in the transport of synthesized PG to subcellular compartments taking part in GAG modifications.

Apart from alterations in the metabolism of small fascia PGs connected with Dupuytren's disease, age-related remodeling of these glycoproteins was also observed in the case of DF. The latter process was reflected in changes in the molecular masses of intact PG as well as their GAG chain structure. However, the observed alterations resembled those affecting NF-derived proteoglycans during the course of aging.

Connected with Dupuytren's contracture, the alterations in matrix PGs lead to an accumulation of DS and CS in diseased tissue. This latter phenomenon has been reported by others (*33*, *34*). It is worthy of note that similar remodeling of the matrix PG (and matrix GAG) profile has been observed in the case of hypertrophic skin scars (*35*) and scarred fascia lata (*15*), demonstrating the existence of common mechanisms involved in some types of wound healing and Dupuytren's disease. However, the alterations in DF matrix PGs are only a part of the disease-associated complex rearrangement of ECM that includes collagen accumulation accompanied by an increase in the type III to type I collagen ratio (*33*), the presence of fibronectin splice-variants (ED-A+ and ED-B+) and its oncofetal glycosylated form (*36*, *37*), and the appearance of molecules commonly found in basal membranes, such as laminin and type IV collagen (*38*). Nevertheless, apart from the above-mentioned changes, matrix PG remodeling can significantly influence ECM properties. For example, decorin via its core protein inhibits the proliferation of many carcinoma cells, including those of connective tissue origin, in a manner involving the up-regulation of p21, an inhibitor of cyclin-dependent kinases (*39*). On the other hand, versican can stimulate fibroblast proliferation (*40*). This effect is promoted by large PG epithelial growth factor–like motifs (*40*). Thus, palmar fascia fibroblast proliferation may depend in part on the decorin to versican ratio. Apart from a direct influence on cell growth, PGs can also modulate growth factor activity. Small leucine-rich PGs (especially decorin) bind *via* their core proteins or GAG chains to many cytokins and growth factors (*41–46*) sequestering them from cell surface receptors. Some of these cytokines and growth factors are also involved in Dupuytren's disease [TGFβ, FGF-2, PDGF (*36*, *47*)]. It seems that the binding of these ligands to DF decorin DS can be promoted due to this GAG oversulfation as well as possibly improved flexibility. This latter property is connected with a higher content of iduronate residues (*48*) in DF decorin DS as compared with normal tissue PG. Moreover, the increased biglycan content in the DF extracellular matrix can also promote growth factor sequestering.

In addition to their influence on cell behaviour, matrix PGs are involved in ECM assembly. For example, collagen fibrogenesis is regulated by some members of the small leucine-rich PG family as judged from studies on PG deficient animals (*49*, *50*). Biglycan knock-out mice show remarkable alterations in collagen fibril morphology, including an increase in the amount of smaller diameter fibrils and less tight fibril packing (*49*, *50*). On the other hand, the appearance of thick collagen fibrils in the mouse decidua is promoted by biglycan (*51*). Although the impact of accumulated biglycan on collagen network arrangement has not been evaluated, it seems that this PG, as a trivalent molecule, may "bridge" adjacent fibrils *via* its two GAG chains and core protein, thus favouring fiber formation. Therefore, it is conceivable that the formation of fibrotic cords typical of late DF (*7*) depends partly on an accumulation of biglycan as we have found in disease affected fascia. Thus, we conclude that the remodeling of palmar fascia matrix PGs may be a significant event in Dupuytren's disease progression from nodular lesions rich in proliferating (myo)fibroblasts to hypocellular fibrotic cords consisting of thick collagen fibers.

REFERENCES

1. Iozzo, R.V. and Murdoch, A.D. (1996) Proteoglycans of the extracellular environment: clues from the gene and protein side offer novel perspectives in molecular diversity and function. *FASEB J.* **10**, 598–614
2. Gallagher, J.T. (2001) Heparan sulfate: growth control with a restricted sequence menu. *J. Clin. Invest.* **108**, 357–361
3. Prydz, K. and Dalen, K.T. (2000) Synthesis and sorting of proteoglycans. *J. Cell Sci.* **113**, 193–205
4. Tiedemann, K., Malmstrom, A., and Westergren-Thorsson, G. (1997) Cytokine regulation of proteoglycan production in fibroblasts: separate and synergistic effects. *Matrix Biol.* **15**, 469–478
5. Westergren-Thorsson, G., Schmidtchen, A., Sarnstrand, B., Fransson, L.A., and Malmstrom, A. (1992) Transforming growth factor-β induces selective increase of proteoglycan production and changes in the copolymeric structure of dermatan sulphate in human skin fibroblasts. *Eur. J. Biochem.* **205**, 277–286
6. Wegrowski, Y., Gillery, P., Kotlarz, G., Perreau, C., Georges, N., and Maquart, F.X. (2000) Modulation of sulfated glycosaminoglycan and small proteoglycan synthesis by the extracellular matrix. *Mol. Cell. Biochem.* **205**, 125–131
7. Rayan, G.M. (1999) Clinical presentation and types of Dupuytren's disease. *Hand Clin.* **15**, 87–96
8. Badalamente, M.A. and Hurst, L.C. (1999) The biochemistry of Dupuytren's disease. *Hand Clin.* **15**, 35–42
9. Tomasek, J.J., Vaughan, M.B., and Haaksma, C.J. (1999) Cellular structure and biology of Dupuytren's disease. *Hand Clin.* **15**, 21–34
10. Murrell, G.A.C. (1991) The role of the fibroblast in Dupuytren's contracture. *Hand Clin.* **7**, 669–680
11. Rombouts, J.J., Noel, H., Legrain, Y., and Munting, E. (1989) Prediction of recurrence in the treatment of Dupuytren's disease: Evaluation of a histologic classification. *J. Hand Surg.* **14**, 644–652
12. Farndale, R.W., Buttle, D.J., and Barrett, A.J. (1986) Improved quantitation and discrimination of sulphated glycosaminoglycans by use of dimethylmethylene blue. *Biochim. Biophys. Acta* **883**, 173–177
13. Bradford, M.M. (1976) A rapid and sensitive method for the quantitation of microgram quantities of protein utilizing the principle of protein-dye binding. *Anal. Biochem.* **72**, 248–254
14. Choi, H.U., Johnson, T.L., Pal, S., Tang, L.H., Rosenberg, L., and Neame, P.J. (1989) Characterization of the dermatan sulfate proteoglycans, DS-PG I and DS-PG II, from bovine articular cartilage and skin isolated by octyl-Sepharose chromatography. *J. Biol. Chem.* **264**, 2876–2884
15. Koźma, E.M., Olczyk, K., Głowacki, A., and Bobiński, R. (2000) An accumulation of proteoglycans in scarred fascia. *Mol. Cell. Biochem.* **203**, 103–112
16. Laemmli, U.K. (1970) Cleavage of structural proteins during the assembly of the head of bacteriophage T4. *Nature* **227**, 680–685
17. Krueger, R.C. and Schwartz, N.B. (1987) An improved method of sequential Alcian blue and ammoniacal silver staining of chondroitin sulfate proteoglycans in polyacrylamide gels. *Anal. Biochem.* **167**, 295–300

18. Koźma, E.M., Olczyk, K., and Głowacki, A. (2001) Dermatan sulfates of normal and scarred fascia. *Comp. Biochem. Physiol. Part B* **128**, 221–232
19. Blumenkrantz, N. and Asboe-Hansen, G. (1973) New method for quantitative determination of uronic acids. *Anal. Biochem.* **54**, 484–489
20. Lyon, M. and Gallagher, J.T. (1990) A general method for the detection and mapping of submicrogram quantities of glycosaminoglycan oligosaccharides on polyacrylamide gels by sequential staining with azur A and ammoniacal silver. *Anal. Biochem.* **185**, 63–70
21. Carrino, D.A., Sorrell, J.M., and Caplan, A.I. (2000) Age-related changes in the proteoglycans of human skin. *Arch. Biochem. Biophys.* **373**, 91–101
22. Rosenberg, L.C., Choi, H.U., Tang, L.H., Johnson, T.L., Pal, S., Webber, C., Reiner, A., and Poole, R. (1985) Isolation of dermatan sulfate proteoglycans from mature bovine articular cartilages. *J. Biol. Chem.* **260**, 6304–6313
23. Hampson, I.N. and Gallagher, J.T. (1984) Separation of radiolabelled glycosaminoglycan oligosaccharides by polyacrylamide-gel electrophoresis. *Biochem. J.* **221**, 697–705
24. Gu, K., Linhardt, R.J., Laliberte, M., and Zimmermann, D.R. (1995) Purification, characterization and specificity of chondroitin lyases and glucuronidases from *Flavobacterium heparinum*. *Biochem. J.* **312**, 569–577
25. Plaas, A.H.K., Wong-Palms, S., Koob, T., Hernandez, D., Marchuk, L., and Frank, C.B. (2000) Proteoglycan metabolism during repair of the ruptured medial collateral ligament in skeletally mature rabbits. *Arch. Biochem. Biophys.* **374**, 35–41
26. Glossl, J., Beck, M., and Kresse, H. (1984) Biosynthesis of proteodermatan sulfate in cultured human fibroblasts. *J. Biol. Chem.* **259**, 14144–14150
27. Kokenyesi, R. and Silbert, J.E. (1997) Immortalized, cloned mouse chondrocytic cells (MC615) produce three different matrix proteoglycans with core-protein-specific chondroitin/dermatan sulphate structures. *Biochem. J.* **327**, 831–839
28. Seidler, D.G., Breuer, E., Grande-Allen, K.J., Hascall, V.C., and Kresse, H. (2002) Core protein dependence of epimerization of glucuronosyl residues in galactosaminoglycans. *J. Biol. Chem.* **277**, 42409–42416
29. Tufvesson, E., Malmstrom, J., Marko-Varga, G., and Westergren-Thorsson, G. (2002) Biglycan isoforms with differences in polysaccharide substitution and core protein in human lung fibroblasts. *Eur. J. Biochem.* **269**, 3688–3696
30. Sakko, A.J., Ricciardelli, C., Mayne, K., Tilley, W.D., LeBaron, R.G., and Horsfall, D.J. (2000) Versican accumulation in human prostatic fibroblast cultures is enhanced by prostate cancer cell-derived transforming growth factor β1. *Cancer Res.* **61**, 926–930
31. Hart, G.H. (1992) Glycosylation. *Curr. Opin. Cell Biol.* **4**, 1017–1023
32. Silbert, J.E. and Sugumaran, G. (2002) Biosynthesis of chondroitin/dermatan sulfate. *IUBMB Life* **54**, 177–186
33. Bazin, S., Le Lous, M., Duance, V.C., Sims, T.J., Bailey, A.J., Gabbiani, G., D'Andiran, G., Pizzolato, G., Browski, A., Nicoletis, C., and Deaunay, A. (1980) Biochemistry and histology of the connective tissue of Dupuytren's disease lesions. *Eur. J. Clin. Invest.* **10**, 9–16
34. Tunn, S., Gurr, E., and Delbruck, A. (1988) The distribution of unsulphated and sulphated glycosaminoglycans in palmar fascia from patients with Dupuytren's disease and healthy subjects. *J. Clin. Chem. Clin. Biochem.* **26**, 7–14
35. Scott, P.G., Dodd, C.M., Tredget, M.M., Ghahary, A., and Rahemtulla, F. (1996) Chemical characterization and quantification of proteoglycans in human post-burn hypertrophic and mature scars. *Clin. Sci. (Lond.)* **90**, 417–425
36. Berndt, A., Kosmehl, H., Mandel, U., Gabler, U., Luo, X., Celeda, D., Zardi, L., and Katenkamp, D. (1995) TGFβ and bFGF synthesis and localization in Dupuytren's disease (nodular palmar fibromatosis) relative to cellular activity, myofibroblast phenotype and oncofetal variants of fibronectin. *Histochem. J.* **27**, 1014–1020
37. Kosmehl, H., Berndt, A., Katenkamp, D., Mandel, U., Bohle, R., Gabler, U., and Celeda, D. (1995) Differential expression of fibronectin splice variants, oncofetal glycosylated fibronectin and laminin isoforms in nodular palmar fibromatosis. *Pathol. Res. Pract.* **191**, 1105–1113
38. Berndt, A., Kosmehl, H., Katenkamp, D., and Tauchmann, V. (1994) Appearance of the myofibroblastic phenotype in Dupuytren's disease is associated with a fibronectin, laminin, collagen type IV and tenascin extracellular matrix. *Pathobiology* **62**, 55–58
39. Santra, M., Mann, D.M., Mercer, E.W., Skorski, T., Calabretta, B., and Iozzo, R.V. (1997) Ectopic expression of decorin protein core causes a generalized growth suppression in neoplastic cells of various histogenetic origin and requires endogenous p21, an inhibitor of cyclin-dependent kinases. *J. Clin. Invest.* **100**, 149–157
40. Zhang, Y., Cao, L., Yang, B.L., and Yang, B.B. (1998) The G3 domain of versican enhances cell proliferation via epidermial growth factor-like motifs. *J. Biol. Chem.* **273**, 21342–21351
41. Hildebrand, A., Romaris, M., Rasmussen, L.M., Heinegard, D., Twardzik, D.R., Border, W.A., and Ruoslahti, E. (1994) Interaction of the small interstitial proteoglycans biglycan, decorin and fibromodulin with transforming growth factor beta. *Biochem. J.* **302**, 527–534
42. Tufvesson, E. and Westergren-Thorsson, G. (2002) Tumour necrosis factor-α interacts with biglycan and decorin. *FEBS Lett.* **530**, 124–128
43. Penc, S.F., Pomahac, B., Winkler, T., Dorschner, R.A., Eriksson, E., Herndorn, M., and Gallo, R.L. (1998) Dermatan sulfate released after injury is a potent promoter of fibroblast growth factor-2 function. *J. Biol. Chem.* **273**, 28116–28121
44. Lyon, M., Deakin, J.A., Rahmoune, H., Fernig, D.G., Nakamura, T., and Gallagher, J.T. (1998) Hepatocyte growth factor/scatter factor binds with high affinity to dermatan sulfate. *J. Biol. Chem.* **273**, 271–278
45. Trowbridge, J.M., Rudisill, J.A., Ron, D., and Gallo, R.L. (2002) Dermatan sulfate binds and potentiates activity of keratinocyte growth factor (FGF-7). *J. Biol. Chem.* **277**, 42815–42820
46. Fager, G., Camejo, G., Olsson, U., Ostergren-Lunden, G., Lustig, F., and Bonjers, G. (1995) Binding of platelet-derived growth factor and low density lipoproteins to glycosaminoglycan species produced by human arterial smooth muscle cells. *J. Cell Physiol.* **163**, 380–392
47. Badalamente, M.A., Hurst, L.C., and Sampson, S.P. (1992) Platelet-derived growth factor in Dupuytren's disease. *J. Hand Surg. (Am)* **17**, 317–323
48. Casu, B., Ferro, D.R., Ragazzi, M., and Torri, G. (1993) Conformation of iduronic acid-containing glycosaminoglycans in *Dermatan Sulphate Proteoglycans Chemistry*, *Biology*, *Chemical Pathology* (Scott, J.E., ed.) pp. 41–53, Portland Press, London and Chapel Hill
49. Ameye, L., Aria, D., Jepsen, K., Oldberg, A., Xu, T., and Young, M.F. (2002) Abnormal collagen fibrils in tendon of biglycan/fibromodulin-deficient mice lead to gait impairment, ectopic ossification, and osteoarthritis. *FASEB J.* **16**, 673–680
50. Corsi, A., Xu, T., Chen, X-D. Boyde, A., Liang, J., Mankani, M., Sommer, B., Iozzo, R.V., Eichstetter, I., Gehron Robey, P., Bianco, P., and Young, M.F. (2002) Phenotypic effects of biglycan deficiency are linked to collagen fibril abnormalities, are synergized by decorin deficiency, and mimic Ehlers-Danlos-like changes in bone and other connective tissues. *J. Bone Miner. Res.* **17**, 1180–1189
51. San Martin, S. and Zorn, T.M.T. (2003) The small proteoglycan biglycan is associated with thick collagen fibrils in the mouse decidua. *Cell. Mol. Biol.* **49**, 673–678